A Method for Describing the Stress and Strain Dependency of Stiffness in Sand

Méthode de description des effets des contraintes et déformations sur la rigidité du sable

R. Whittle
Cambridge Insitu Ltd, U.K.
L. Liu
Mott MacDonald Ltd, U.K.

ABSTRACT:High resolution pressuremeters are used routinely to provide stiffness parameters from unload/reload cycles. This technique is largely unaffected by disturbance and so can be used with all insertion modes. It is straightforward to describe the strain dependency of stiffness in clays in the range 10^{-4} to 10^{-2} using a power law to fit the trend of reloading data (Bolton & Whittle, 1999). Pressuremeter tests in clay tend to be undrained and following failure the mean effective stress throughout the loading is constant. Hence all cycles plot the same trend, a rare example of repeatability in a destructive test.

Pressuremeter tests in sand are drained events. Consequently the mean effective stress changes throughout the loading, so in addition to strain dependency there is stress dependency. The method outlined in this paper results in a single expression that describes the strain and stress development of stiffness. This is done by combining a power law approach with a widely used stress level adjustment (Janbu, 1963). The only requirement from the test is that there should be at least three unload/reload cycles.

RÉSUMÉ : les pressiomètres à haute résolution sont couramment utilisés pour relever les paramètres de rigidité sur les cycles de déchargement/rechargement. Cette technique n'est, pour l'essentiel, pas affectée par les perturbations et peut donc être utilisée avec tous les modes d'insertion. Les effets des déformations sur la rigidité des argiles dans la gamme 10^{-4}-10^{-2} se décrivent de façon simple, en utilisant une loi de puissance pour lisser la tendance des données de rechargement (Bolton & Whittle, 1999). Les essais pressiométriques réalisés dans l'argile sont généralement non drainés et, en cas de défaillance, la contrainte effective moyenne est constante sur l'ensemble de la charge. Cela explique pourquoi tous les cycles tracent la même tendance, exemple rare de répétitivité pour des essais destructifs.

Les essais pressiométriques effectués dans le sable sont des événements drainés. Cela induit des variations de la contrainte effective moyenne sur l'ensemble de la charge : il y a donc, en plus de la dépendance aux déformations, une dépendance aux tensions. La méthode proposée dans cet article permet d'obtenir une expression unique pour décrire les effets des déformations et des tensions sur la rigidité. Cela passe par la combinaison entre une approche fondée sur la loi des puissances et une pratique, largement utilisée, d'ajustement du niveau de contrainte (Janbu, 1963). La seule exigence du test est la nécessité de disposer d'au moins trois cycles de déchargement/rechargement.

KEYWORDS: Shear modulus, non-linearity, stress dependency, strain dependency, unload, reload

1 INTRODUCTION

Pressuremeter tests incorporating small cycles of unloading and reloading are able to provide consistent and repeatable data for soil stiffness. The technique was suggested as a procedure for determining shear modulus in the early 1980's (Hughes, 1982).

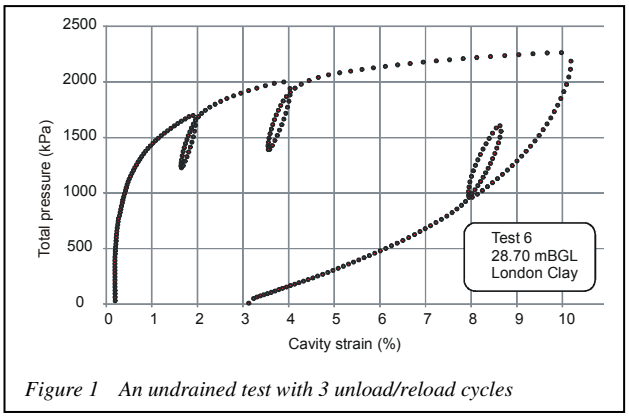

Figure 1 An undrained test with 3 unload/reload cycles

The overwhelming advantage of the procedure over other ways of deriving stiffness parameters from a cavity expansion test is the relative immunity from insertion effects. The only requirement for the procedure is that a well-developed plastic condition exists before a cycle is taken. Any pressuremeter able to load the material to a greater stress than it has previously suffered has the potential to deliver highly repeatable data for stiffness. There is no intrinsic advantage in using self-boring over more invasive techniques such as pre-boring or pushing.

Reloading cycles are characterised by a small change in displacement for a comparatively large stress alteration, so the technique demands good resolution of displacement and a low level of uncertainty in the measurement. Uncertainty can result from mechanical imperfections in the displacement system (friction), the finite stiffness of the pressuremeter (compliance) and the perverse nature of the ground itself. A cycle involves two changes of loading direction and most materials will not tolerate this without some level of creep. Figure 1 shows a

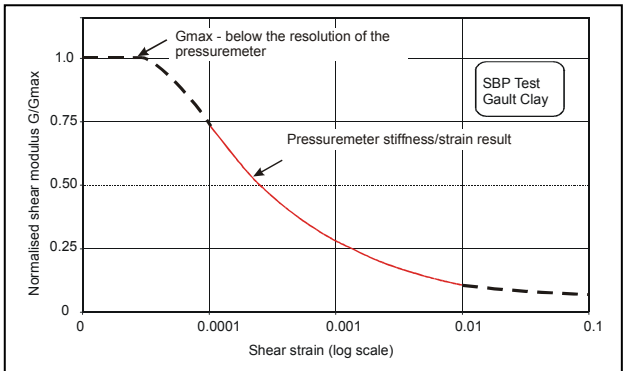

Figure 2 The strain range of pressuremeter stiffness

typical test in clay incorporating three cycles, including one on the final unloading.

The unload/reload cycles (or 'loops') do not follow a linear path but appear hysteretic. This hysteresis is not a defect but a characteristic of the non-linear nature of the underlying stress:strain properties of the material under load. If the resolution of the system is sufficiently high then the path followed during an unload/reload event can be used to resolve the strain dependency of stiffness over a shear strain variation of 10^{-4} to 10^{-2}. The lower end of this scale is not quite small enough to capture the maximum stiffness of the material but the range is sufficient to describe the greater part of the degradation curve (fig 2).

There are a number of methods for using unload/reload data to obtain the degradation trend (Muir Wood 1990, Jardine, 1991) but a method widely used for undrained tests is that outlined by Bolton & Whittle, 1999. This assumes that the stress:strain degradation follows a simple power law, showing that secant shear modulus G_s is given by

$$G_s = \alpha\gamma^{(\beta-1)} \qquad (1)$$

where α and β are the constant and exponent of the power law trend of shear stress against shear strain.

γ is any shear strain in the range 10^{-4} to 10^{-2}

Pressuremeters do not measure shear stress and shear strain directly. To determine non-linear stiffness parameters, devices must be able to resolve displacements of a micron or less. These will be probes that have local instrumentation and give readings of the pressure and displacement of the cavity wall, in effect

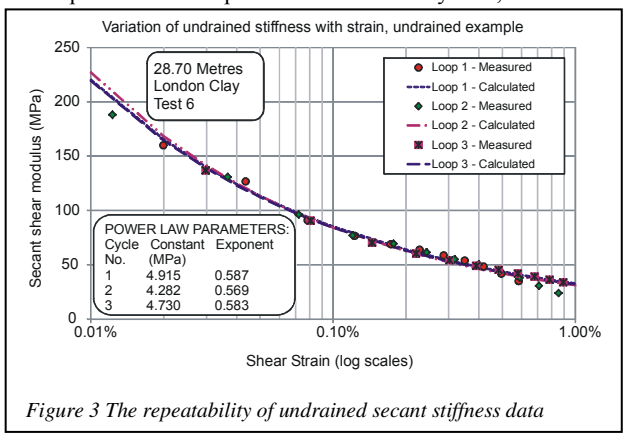

Figure 3 The repeatability of undrained secant stiffness data

radial stress σ_r and circumferential strain ε_c. The method for

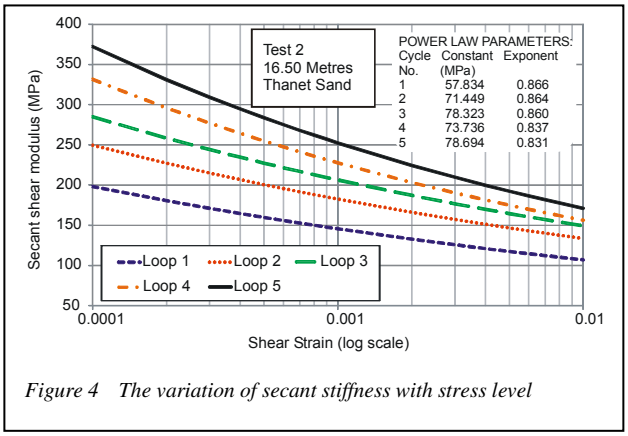

Figure 4 The variation of secant stiffness with stress level

obtaining α and β from σ_r and ε_c co-ordinates is briefly described in section 2. A similar exponential trend is evident when unload/reload cycles are conducted in drained material but the calculations for shear stress and shear strain are less familiar and are more complex (section 3).

Although the power law approach can be considered as merely curve fitting, there are reasons for thinking that the splitting and crushing of particles at the micro-mechanical scale with the consequent redistribution of stress must result in an exponential trend as soil is loaded past its linear elastic range (Bolton 1999). The exponent β seems to have a physical meaning, related to average particle size at the micro-mechanical scale. A typical clay will have a β in the range 0.5 to 0.6, a dense sand in the range 0.8 to 0.9. A β of 1, meaning linear elasticity, then emerges as a characteristic of an intact material (rock).

The current stiffness at any point in a pressuremeter loading is also stress dependent. Undrained events have the convenient feature that the mean effective stress is constant following failure, so that to a first approximation all cycles give similar data (fig 3). In the case of drained events the mean effective stress changes throughout the loading and there is a corresponding alteration in stiffness (fig 4). Bellotti et al (1989) give a procedure that allows pressuremeter determined modulus to be normalised to a common stress level such as the effective insitu lateral stress, σ'_{ho} . This paper uses much of the argument but offers a different solution that allows stress and strain dependency to be defined with one expression. It starts by reviewing a method already used for tests in clay, and then adapting it for tests in sand.

2 Undrained analysis

For each cycle, co-ordinates of radial pressure and displacement are plotted on axes of radial stress σ_r and circumferential strain ε_c (fig 5). Each half of the unload/reload cycle is a product of the same stress:strain properties so it is only necessary to plot data following the loop turnabout point. These are least affected by mechanical imperfections and material creep. An origin is identified at the turnaround point; all subsequent data are plotted from this origin and the power law trend is obtained by regression analysis. As the example shows, the correlation coefficient is remarkably good.

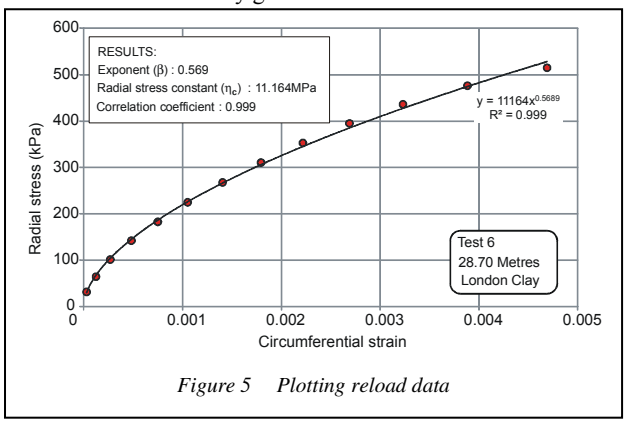

Figure 5 Plotting reload data

The constant and exponent define a power law in radial stress/circumferential strain space. Because the test is undrained and there are no volumetric strains to consider, the equivalent power law terms in radial stress and shear strain space is just a translation of the abscissa and so can be calculated by dividing the constant term η_c by 2^β to give η_s. This relationship holds for shear strains below the yield strain. Palmer 1972 is an exact solution that defines the current shear stress τ in terms of the current gradient of a pressuremeter curve:

$$\tau = \gamma \frac{dp}{d\gamma} \qquad (2)$$

where p is radial stress at the cavity wall
γ is shear strain

Strictly, this is a small strain version of the solution but for the strain range being considered this is not significant. The procedure is as follows:

From the power law obtained from fig 5:

$$p = \eta_c \varepsilon_c^{\beta} \qquad (3)$$

Modify the coefficient to obtain the equivalent expression in terms of shear strain:

$$p = (\eta_c \varepsilon_c^{\beta})/2^{\beta} = \eta_s \gamma^{\beta} \qquad (4)$$

Substitute for p in (2) with the power law result to solve the partial differential equation and divide by shear strain to give secant shear modulus :

$$\tau = \gamma\left(\beta\eta_s\gamma^{\beta-1}\right) = \beta\eta_s\gamma^{\beta} \qquad (5)$$

$$\frac{\tau}{\gamma} = \beta\eta_s\gamma^{\beta-1} = G_s \qquad (6)$$

where $\beta\eta_s = \alpha$, the shear stress coefficient

(6) is identical to (1). The typical result shown in fig.3 shows smooth lines defined by the power law and points obtained by applying the Palmer result (2) directly to the measured data.

3 Drained analysis – strain dependency

Initially, drained unload/reload data are treated in a similar way to undrained data. For each cycle a plot of radial stress against circumferential strain is produced and fitted with a power law, the one change being that the ordinate is now *effective* radial stress. The result is a power curve relating stress to strain at the cavity wall in the following form:

$$p' = \eta_c \varepsilon_c^{\beta} \qquad (7)$$

(7) may be used to solve the numerical solution for a drained cavity expansion of a purely frictional material due to Manassero (1989). Some additional information about the material is required, specifically the water table (to allow total stress to be converted to effective stress) and an estimate of the internal angle of friction when the material is deforming at constant volume. The Manassero solution uses Rowe's stress dilatancy theory and relates the unknown current radial strain ε_r to the known current gradient of a loading curve in radial stress/circumferential strain space via the stress ratio K_a :

$$k_a^{cv} \text{ is } \frac{1-\sin\varphi_{cv}}{1+\sin\varphi_{cv}} \qquad (8)$$

and Φ_{cv} is the internal angle of friction when thematerial is deforming at constant volume.

Knowing the co-ordinates of two adjacent positions on the loading curve, (i) and (i-1), the radial strain at (i) can be found as follows:

$$\varepsilon_R(i) = \frac{p(i)[\varepsilon_C(i-1) + k_a^{cv}\varepsilon_R(i-1)] - p(i-1)\varepsilon_C(i)}{2[p(i)(1+k_a^{cv}) - p(i-1)}} + \frac{p(i)[\varepsilon_C(i-1) - \varepsilon_R(i-1)] + p(i-1)[\varepsilon_R(i-1)(1+k_a^{cv}) - \varepsilon_C(i)}{2k_a^{cv}\,p(i-1)} \qquad (9)$$

Because the reloading data are referred to a new origin at the loop turn-around co-ordinate, the radial strain starts from zero. The first interval can be calculated and the sequence of dependent calculations started. Given radial strain, the unknown circumferential stress is straightforward to derive.

Manassero acknowledges that measured data are likely to be too noisy to be used directly and suggests curve fitting the cavity expansion prior to implementing the solution. The approach here is in effect to curve fit the elastic parts of the loading (the unload/reload cycles). A smooth set of radial stress and circumferential strain co-ordinates are produced and used with (9) to derive an equivalent set of radial strains. It is then straightforward to obtain the trend of shear strain and shear stress, another power law. This gives α and a modified β. A typical test in dense sand is shown in fig.6 and the resulting stiffness:strain curves are shown in fig.4. In general β values from the shear stress/shear strain data are very slightly greater (tending more towards 1, the linear elastic value) than those obtained from the initial power law, suggesting small volumetric strains are being generated during the unload/reload events.

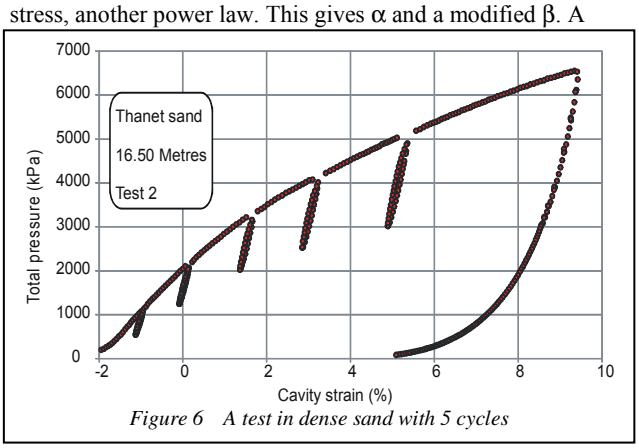

Figure 6 A test in dense sand with 5 cycles

4 Drained analysis – stress dependency

Bellotti et al (1989) give a procedure for converting modulus at intermediate stress levels to a reference level, the insitu effective stress σ'_{ho}. It is based on the relationship proposed by Janbu 1963:

$$G_{ref} = G_{meas}\left(\frac{\sigma'_{ho}}{\sigma_{av}}\right)^n \qquad (10)$$

The exponent n is assumed to be constant for a particular material. The plane strain mean effective stress is defined as $\sigma_{av} = \frac{1}{2}(\sigma_r' + \sigma_c')$. Throughout an elastic unload/reload event the mean effective stress remains constant as changes in radial stress are matched by equivalent changes in the circumferential stress Assuming that plasticity has been initiated, then σ_r' at the cavity wall is p' and is measured, and σ_c' is related via $\sigma_c' = \sigma_r'(1+1/N)$ where N is the principal stress ratio $[1+\sin\Phi]/[1-\sin\Phi]$. Φ is the peak angle of internal friction. It follows that at the commencement of an unload/reload cycle:

$$\sigma_{AV} = \left(\frac{p'}{1+\sin\phi}\right) \qquad (11)$$

Bellotti *et al* use a more complex calculation to derive σ_{av} that reflects an average of all values from the cavity wall to the elastic boundary but the stress level at the borehole wall is the dominant factor. In principle the exponent n can be obtained by plotting mean effective stress against the measured modulus. However the exponent is not just a stress related variable, it also

varies with strain so for a good correlation the measured modulus data would have to use the same strain amplitude.

Table 1 extracts data from the test shown in fig.6. The values of α and β are those shown in fig 4 and the mean effective stress has been calculated from (11). It happens that for this test the ambient pore water pressure was zero so total and effective radial stress are the same:

Table 1 Unload/reload data from 5 cycles in dense sand

Cycle	Constant α	Exponent β	p´	σ_{av}
	(MPa)		(kPa)	(MPa)
1	57.834	0.866	1075	0.649
2	71.449	0.864	2102	1.269
3	78.323	0.860	3216	1.942
4	73.736	0.837	4077	2.462
5	78.694	0.831	5050	3.049
Ambient pore water pressure is zero and the internal angle of friction is 41°				

Figures 7 and 8 show how the limitations of (10) can be overcome and the strain dependency of the stress level relationship extracted. The α and β values in Table 1 are used to give estimates of secant shear modulus over a sensible strain

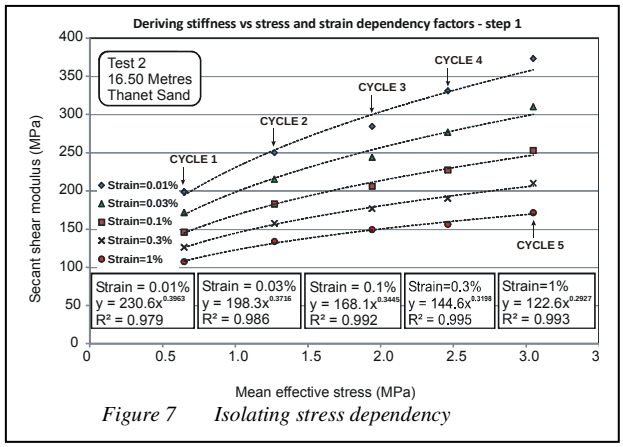

Figure 7 Isolating stress dependency

range. Figure 7 is the result, where each cycle is controlled by a particular stress level and contributes 5 modulus values at steps of strain between 0.01% and 1%. For each strain level the best fit power curve is found and the results are listed in Table 2.

Table 2 - Constant and exponent of stress and strain dependency

Strain level	Coefficient (MPa)	Exponent	Regression Coefficient
0.01%	230.6	0.3963	0.98
0.03%	198.3	0.3716	0.99
0.10%	168.1	0.3445	0.99
0.30%	144.6	0.3198	0.99
1.00%	122.6	0.2927	0.99

Step 2 of this process is to isolate the influence of strain. Figure 8 shows the coefficient and exponent of the exponential curves obtained in figure 7 plotted against strain. The log lines that best define the development of the constant values and exponent values are obtained (see table 3), where log strain is the abscissa.

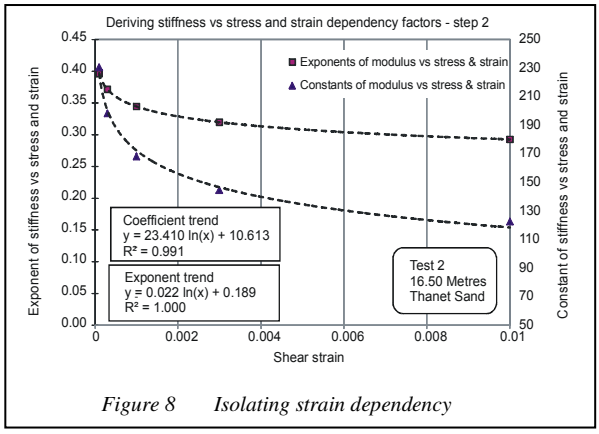

Figure 8 Isolating strain dependency

Table 3 - Final parameters for stress and strain dependency

	Coeff.	Const.
Values for the exponent of modulus as a function of log strain (*x* and *z*)	-0.022	0.189
Values for the constant of modulus as a function of log strain (*c* and *d*)	-23.41	10.613

The single power curve defining secant shear modulus for this material using the results listed in Table 3 is written as follows, where the coefficient and exponent vary with shear strain:

$$G_s = A\sigma_{av}^{J} \quad (12)$$

where

$$A = c\ln(\gamma) + d$$

$$J = x\ln(\gamma) + z$$

The efficacy of the solution can be demonstrated graphically (fig.9) by comparing the starting parameters used to make fig 7 to those obtained using the final result. The lines in the plot are

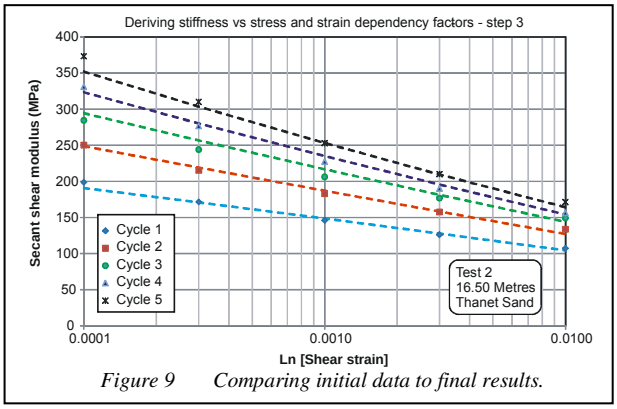

Figure 9 Comparing initial data to final results.

obtained from applying the solution to the values of σ_{av} given in Table 1.

5 Discussion and conclusions

There are many ways of obtaining shear stress and shear strain parameters from a pressuremeter test, but none which require so little external information as the method outlined here. For the most part all the information necessary to produce the factors for (12) comes directly from the measured field curve.

There is a need to know the ambient pore water pressure and the critical state friction angle and also the peak angle of internal friction, Φ_{pk}. To some extent, therefore, the factors are

influenced by the analysis of the whole test curve. However the exponent J defined in (12) is unaffected by changes to Φ_{pk} – it is only the coefficient A that is slightly altered, so major changes in Φ_{pk} have a minor influence on G_s. The approach to deriving the mean effective stress is about the simplest possible, and depends on Φ_{pk} being constant over the part of the test curve where the unload/reload cycles are taken.

If volumetric strains are ignored whilst the sand is deforming elastically, then shear stress and shear strain co-ordinates from unload/reload cycles could, for simplicity, be derived using the Palmer solution for undrained events. The effect is to slightly over-estimate stiffness, the magnitude of the error depending on how far away the sand is from its critical state. The Manassero method gives a rigorously correct solution for shear strains below the plastic threshold.

Pressuremeter tests are shearing processes and the deformations and stresses measured are a function of the shear stiffness of the material. Throughout this description plane strain has been used but it is a simple matter to derive equivalent expressions for axial strain and to include Poisson's ratio to allow Young's modulus to be inferred (Whittle 1999). The shear modulus being determined is G_{hh} so all extrapolations between this value and other kinds of modulus need to consider the anisotropy of the material.

Although not given here, it is straightforward to adapt (11) for the case of a drained expansion in a c′ - phi material, and to calculate σ_{av} for plastic contraction.

The method that has been given is the reduction of a number of power curves until a single expression is obtained that defines secant shear modulus as a function of mean effective stress. For the most part the stress of most interest will be the effective insitu lateral stress, σ'_{ho}. One of the pleasing aspects of the relationship described is the absence of a need to know σ'_{ho} in order to derive all the parameters.

The method has a possible application in finite element code. It is common practice for consultancies to use non-linear modelling and the solution presented here allows fine control of stress and strain level for describing stiffness variation. A considerable amount of calibration and back analysis would be required to validate the model.

6 Terminology

A Stress level coefficient with a strain dependency

ε strain, suffix r for radial stress, c for circumferential stress

γ shear strain

p pressure at the cavity wall

G_s secant shear modulus

Φ_{pk} peak angle of internal friction.

Φ_{cv} angle of internal friction when the material is shearing at constant volume

σ stress, suffix r for radial stress, c for circumferential stress

σ_{av} Mean effective stress

σ'_{ho} Effective insitu lateral stress

k_p constant volume stress ratio $[1+\sin\phi_{cv}]/[1-\sin\phi_{cv}]$. k_a is $1/k_p$

τ shear stress

α shear stress constant of a power law of stiffness degradation

η radial stress constant of a power law of stiffness degradation – suffix s or c if the abscissa is shear strain or circumferential strain

β exponent of a power law of stiffness degradation

n stress exponent describing the variation of stiffness with stress level for a linear elastic response

J stress exponent, describing the variation of stiffness with stress level incorporating strain dependency

7 References

BELLOTTI, R., GHIONNA, V., JAMIOLKOWSKI, M., ROBERTSON, P. and PETERSON, R. 1989. Interpretation of moduli from self-boring pressuremeter tests in sand. Géotechnique 39, no.2, pp.269-292.

BOLTON M.D. 1999. The Role of Micro-Mechanics in Soil Mechanics.CUED/D-Soils/TR313

BOLTON M.D. and WHITTLE R.W. 1999. A non-linear elastic/perfectly plastic analysis for plane strain undrained expansion tests. Géotechnique 49, No. 1, pp 133-141.

HUGHES, J.M.O., 1982. Interpretation of pressuremeter tests for the determination of elastic shear modulus. Proc. Eng. Fdn. Conf. Updating Subsurface Sampling of Soils and Rocks and their InSitu Testing, Santa Barbara, Balkema, Rotterdam, pp. 279– 289.

JANBU, N. 1963. Soil compressibility as determined by oedometer and triaxial tests. Proc. 3rd Eur. Conf. Soil Mech., Wiesbaden 2, pp 19-24.

JARDINE, R.J. 1991. Discussing 'Strain-dependent moduli and pressuremeter tests' . Géotechnique 41, No. 4.,pp 621-624

MANASSERO, M. 1989. Stress-Strain Relationships from Drained Self Boring Pressuremeter Tests in Sand. Géotechnique 39, No.2, pp 293-307.

MUIR WOOD, D. 1990. Strain dependent soil moduli and pressuremeter tests. Géotechnique, 40, pp 509-512.

PALMER, A.C. 1972. Undrained plane-strain expansion of a cylindrical cavity in clay: a simple interpretation of the pressuremeter test, Géotechnique 22 No. 3 pp 451- 457.

ROWE, P.W. 1962.. The Stress Dilatancy Relation for Static Equilibrium of an Assembly of Particles in Contact. Proceedings of the Royal Society. Vol. 269, Series A, pp 500-527.

WHITTLE, R.W 1999. Using non-linear elasticity to obtain the engineering properties of clay. Ground Engineering, May, vol. 32, no.5, pp 30-34.